J Solid State Electrochem (2007) 11:1335–1346
DOI 10.1007/s10008-007-0296-2

ORIGINAL PAPER

Electrochemical monitoring of indigo preparation using Maya's ancient procedures

Antonio Doménech · María Teresa Doménech-Carbó · María Luisa Vázquez de Agredos Pascual

Received: 26 January 2007 / Revised: 9 February 2007 / Accepted: 15 February 2007 / Published online: 8 March 2007

Abstract The preparation of indigo from *Indigofera suffruticosa* following the procedures attributed to ancient Mayas was electrochemically monitored using the voltammetry-of-microparticles approach. The mechanism formation of indigotin and indirubin from its precursors, indican and isatan, is discussed. Comparison of voltammetric profiles for differently prepared and commercial indigos and genuine Maya Blue samples suggests that the preparation procedure of indigo changed during the Late Classical Maya period.

Keywords Maya Blue · Indigo · Indirubin · Synthesis · Electrochemistry

Electronic supplementary material The online version of this article (doi:10.1007/s10008-007-0296-2) contains supplementary material, which is available to authorized users.

A. Doménech (✉)
Departament de Química Analítica, Universitat de València,
Dr. Moliner, 50,
46100 Burjassot (València), Spain
e-mail: antonio.domenech@uv.es

M. T. Doménech-Carbó · M. L. V. de Agredos Pascual
Institut de Restauració del Patrimoni/Departament de Conservació i Restauració de Bens Culturals,
Universitat Politécnica de València,
Camí de Vera 14,
46022 València, Spain

M. L. V. de Agredos Pascual
Departament de Historia del Arte, Universitat de València,
Passeig al Mar,
València, Spain

Introduction

The preparation and properties of Maya Blue (MB), a famous pigment produced by the ancient Mayas, has claimed considerable attention recently because of its peculiar colour and enormous stability [1–12]. MB can be described as a nanostructured material resulting from the attachment of an organic molecule, indigo, to a phyllosilicate, palygorskite (or attapulgite), typical of Yucatan.

The organic component of MB is natural indigo, a blue dye widely used in several civilisations as a pigmenting agent. The European source of indigo is *Isatis tinctoria* who replaced progressively the Indian plant *Indigofera tinctoria* since the seventeenth century. In pre-Columbian America, however, *Indigofera suffruticosa* was the main source of indigo used by Mayas and other peoples, being in fact used until recent times [13].

The natural product is mainly formed by indigotin (3H-indol-3-one, 2-(1,3-dihydro-3-oxo-2H-indol-2-ylidene)-1, 2-dihydro) accompanied by indirubin (or indigo brown, 2H-indol-2-one, 3-(1,3-dihydro-3-oxo-2H-indol-2-ylidene)-1,3-dihydro). A related compound is isoindigotin (2H-indol-2-one, 3-(1,2-dihydro-2-oxo-3H-indol-3-ylidene)-1, 3-dihydro). Indigotin and indurubin can eventually be accompanied by precursor compounds, mainly indican (indoxyl-β-D-glucoside) and isatan (A and B) [14–21]. Directly related compounds are isatin (1H-indole-2,3-dione), indoxyl (1H-indol-3-ol) and 2-indolinone [14–21]. The molecular structure of the main species is depicted in Scheme 1.

The reasons for the peculiar hue of MB remain controversial [2–12], being attributed to Mie dispersion in iron and iron oxide nanoparticles [2, 3] or batochromic shift of indigo bands because of its association with the palygorskite matrix [4, 8, 9, 11, 12]. Different models for describing the indigo–palygorskite interaction have been

Scheme 1 Representation of the molecular structures of indican, isatans, isatin and indoxyl

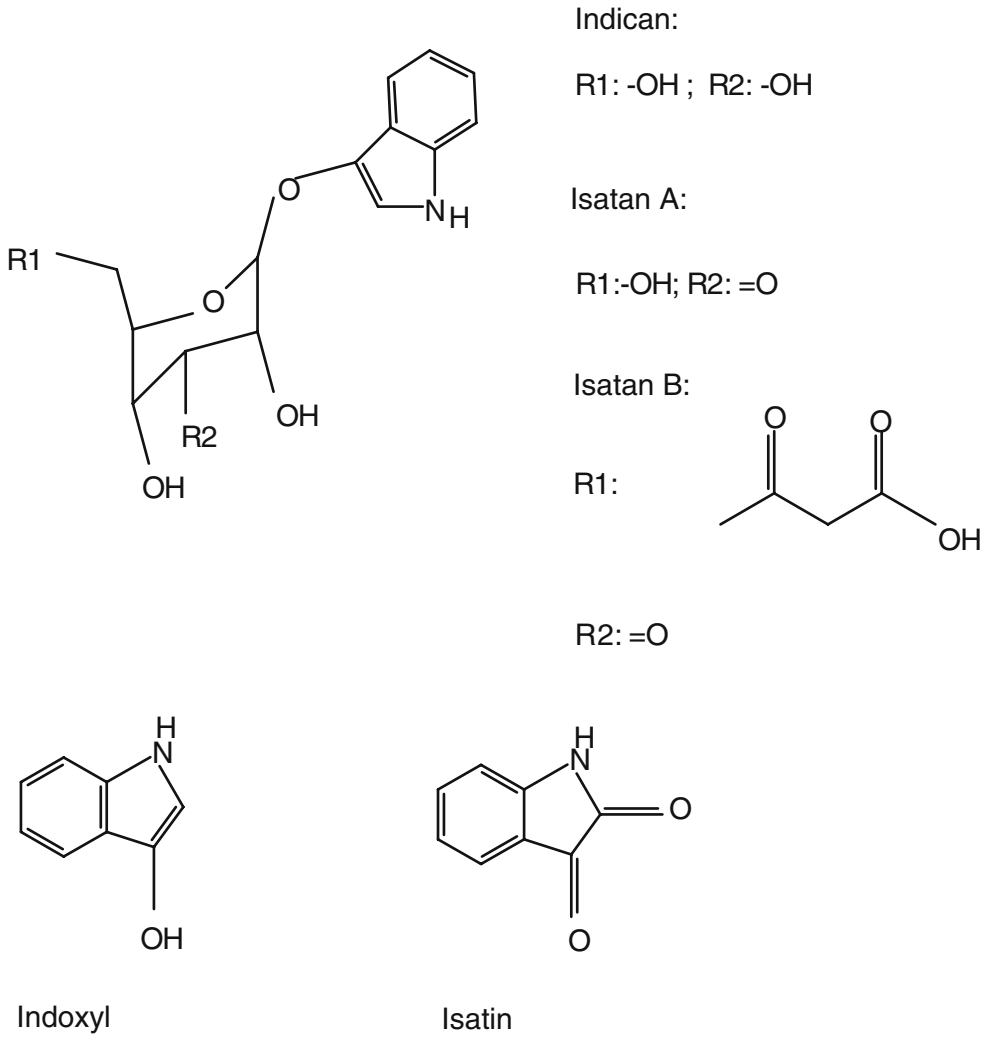

recently proposed by Fois et al. [5], Chiari et al. [4], Giustetto et al. [12] and Hubbard et al. [6].

In this context, we have already reported a physicochemical study on MB samples from different archaeological sites of Yucatan and Campeche. Application of the voltammetry of microparticles (VMP) allows for proposing the presence of the oxidised form of indigo, dehydroindigo, in the pigment [22]. Spectral data [23] indicate that dehydroindigo can contribute significantly to the peculiar hue of MB, so that the ancient Mayas may modulate the colour of the pigment by varying the relative indigo/dehydroindigo proportion in the palygorskite–indigo complex [22].

Dehydroindigo may result presumably from an aerobic oxidation of indigo (1) taking place during the preparation of the dye precursor of MB or (2) via a palygorskite-assisted reaction occurring exclusively within the compartmentalised space provided by the inorganic host. The elucidation of this matter is made difficult by the fact that, although the Maya's method for obtaining indigo from *Indigofera* leaves is known from historical sources, the preparation procedure of MB from indigo is not known [24–27].

Identification of indigo and from pictorial and textile samples can be achieved by means of liquid chromatography [28, 29], gas chromatography/mass spectrometry [30, 31] and micro-Raman spectrometry [32]. Identification and characterisation of indigo precursors from plant extracts is, however, a partially unsolved task. In fact, the structure of Isatan A and B has been only very recently clarified by Oberthür et al. [19] by identifying the major indoxyl glycoside as isatan A (indoxyl-3-O-(6′-O-malonyl-β-D-ribohexo-3-ulanopyranoside) and by correcting the structure of the related isatan B (indoxyl-3-O-β-D-ribohexo-3-ulanopyranoside). In recent works, Gilbert et al. [18] indicated that indican and isatan B are present in different amounts in extracts from *I. tinctoria* and *Indigofera indigotica*, although only indican is detected in the extracts from *Polygonium* spp., whereas Oberthür et al. [21] have studied the seasonal variation of indoxyl glycosides in

woad leaves and the influence of past-harvest treatment in the detected amounts of indigo precursors. Discussions on the biochemical pathway for the synthesis of indigo in plants have been recently reported by Betchold et al. [33], Berry et al. [34] and Ferreira et al. [35].

In this context, we have electrochemically monitored the preparation of indigo from *I. suffruticosa* leaves using materials and methods that reproduce those used by the ancient Mayas, based on a 'wet' synthesis. The preparation procedure is initiated by the maceration of leaves in a quick-lime suspension in cold water. The resulting suspension was submitted to a prolonged aerobic beating in cold water (24–72 h). VMP, a methodology developed by Scholz et al. [36, 37] based on the mechanical transference of solid microparticles to the surface of an inert electrode, was used. This methodology is of particular interest because it does not require extraction or sample pretreatment and provides direct information of the oxidation degree of the compounds [38, 39]. Application of VMP for characterising different organic compounds has been reported [40–46]. As shown in studies concerning the characterisation of anthraquinone [43, 44] and flavonoid dyes [44, 45], VMP allows for a distinction between compounds having subtle structural differences between them. In this context, the voltammetry of synthetic indigo microparticles has been studied by Bond et al. [46], Komorsky-Lovric et al. [42] and Grygar et al. [44].

In this work, VMP of synthetic indigo and related compounds is compared with that of solid products obtained during different stages of the preparation of indigo from leaves of *I. suffruticosa*. To explore the capabilities of the VMP for acquiring analytical information, it was performed in a chemometric study on a series of 30 MB samples from 12 archaeological sites in Yucatán and Campeche. Square wave voltammetry (SQWV) was routinely used for electrochemical measurements because of its inherently high sensitivity and its reluctance to undergo capacitive effects [47].

Experimental

Synthetic indigo (Fluka), indican (Sigma-Aldrich), isatin (Aldrich), indirubin (Sequoia) and commercial indigo from *Isatis tinctoria* (Kremer 36003) and *Indigofera tinctoria* (Kremer 36002) were used for electrode modification without any pretreatment. Indigo from *I. suffruticosa* was prepared following traditional procedures. Acetic acid (HAc, Panreac), sodium acetate (NaAc, Merck) and phosphate buffer (Panreac) were used as supporting electrolytes. Preparation of standards of isatan B followed the method devised by Kokubun et al. [16] by extracting *I. suffruticosa* leaves with boiling water for 5 min, cooling rapidly at room temperature (25 °C) and acidifying with acetic acid (1% final volume). Indirubin was prepared similarly.

Preparation of indigo using Mayas' traditional procedures was performed as follows: 10 g of leaves of *I. suffruticosa* were macerated for 24 h in a 5-g/l aqueous suspension of quick lime. Then, the suspension was filtered with a cotton cloth to remove leaves, clay and lime and vigorously beaten for 48 h. Aliquots of the suspension were taken at intervals of 2, 6, 12, 24, 36 and 48 h during the beating process. One portion of the filtrate (labelled here as 'wet' samples, V-1 to V-6) was dried with filter paper and submitted to electrochemical measurements. A second portion of the filtrate ('dried' samples, VD-1 to VD-6) was air dried and stored in the dark during 1 week, and then electrochemical measurements were performed.

MB samples were taken from wall paintings of 12 archaeological sites in Yucatán (Chacmultún, D'zula, Ek Balam, Acanceh, Kulubá and Mulchic, all of the Late Classical period, Chichén Itzá, corresponding to the Terminal Classical period, and Mayapán, date at the Postclassical period) and three sites in Campeche (Dzibilnocac and El Tabasqueño, Late Classical period, and the Substructures A-3, A-5 and A-6 of the site of Calakmul, corresponding to the Early Classical period, and the Substructure II-C of the same archaeological site, dated in the Late Preclassical period). Few micrograms (5–10 μg) of sample were taken with the help of a microscalpel in all cases.

Paraffin-impregnated graphite electrodes (PIGEs) consist on cylindrical rods of 5 mm diameter of graphite impregnated under vacuum by paraffin. Preparation details are described in [36, 37]. To prepare sample-modified PIGEs, 0.1–1 mg of the material was powdered in an agate mortar and pestle and placed on a glazed porcelain tile forming a spot of finely distributed material and then abrasively transferred to the surface of a PIGE by rubbing the electrode over that spot of sample.

Electrochemical experiments were performed at 298 K in a three-electrode cell under argon atmosphere using a AgCl (3 M NaCl)/Ag reference electrode and a platinum-wire auxiliary electrode. Cyclic and square wave voltammograms (CVs and SQWVs, respectively) were obtained with a CH I420 equipment.

Fourier transform infrared (FTIR)–attenuated total reflection (ATR) spectra of samples and reference materials were obtained with a Vertex 70 Fourier transform infrared spectrometer with a FR-DTGS (fast recovery deuterated triglycine sulphate) temperature-stabilised coated detector. The number of co-added scans was 32, and the resolution was 4 cm^{-1}. Before FT-IR measurements, partial elimination of interfering carbonate in VD samples was eventually performed by treatment with 1 M HCl during 15 min, rinsing and stirring the resulting suspension in water and subsequently drying it in air.

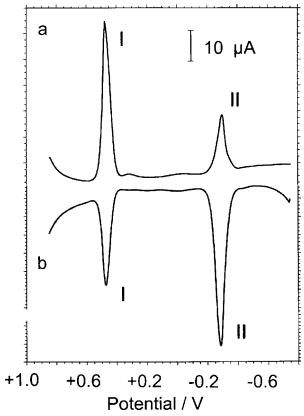

Fig. 1 SQWVs of PIGEs modified with synthetic indigo immersed into 0.50 M HAc+ 0.50 M NaAc buffer at pH 4.85. *a*, Potential scan initiated at +850 mV in the negative direction; *b*, id. at −750 mV in the positive direction. Potential step increment 4 mV; square wave amplitude 25 mV; frequency 15 Hz

Visible spectra were recorded with a Minolta CM-503i spectrophotometer using a Xe-arc lamp and a Si photodiode detector. The instrument was calibrated with a standard white (coordinates Y=95.8; x=0.3167; y=0.3344).

Results and discussion

Electrochemistry of indigo and indigo precursors

The typical SQWV response of indigo-modified electrodes immersed into acetic/acetate buffer is shown in Fig. 1. Two well-defined reversible voltammetric peaks at +470 (I) and −280 mV (II) vs AgCl/Ag, whose peak potentials remain essentially frequency independent. Well-defined anodic and cathodic peaks were obtained upon separate examination of the currents measured in the forward and backward currents of square wave pulses [47], thus denoting that both electrochemical processes behave reversibly. In agreement with literature [42, 44, 46], the voltammetric response of indigo (H_2IN) can be described in terms of its reversible oxidation to dehydroindigo, IN, and reduction to leucoindigo, H_4IN, via two two-proton, two-electron transfer processes. Processes I and II can be represented, respectively, as:

$$H_2IN(s) \rightarrow IN(s) + 2H^+(aq) + 2e^- \quad (1)$$

$$HI_2N(s) + 2H^+(aq) + 2e^- \rightarrow H_4IN(s) \quad (2)$$

where (s) denotes solid phases. Notice that charge conservation is ensured in both cases by the issue/ingress of two protons and two electrons from/to the solid. Molecular structures of dehydroindigo and leucoindigo are illustrated in Scheme 2.

The foregoing voltammetric data can in principle be rationalised on the basis of the model developed by Lovric and Scholz [48, 49] and Oldham [50] for describing the solid-state voltammetry of immobilised microparticles. Following the most recent formulation because of Schröder et al. [51], the redox process starts at the three-phase electrode/electrolyte/microparticle junction. From which, the electrochemical reaction propagates via proton transfer across the electrolyte/particle interface and electron transfer across the electrode/particle interface. The process of

Scheme 2 Redox processes for indigo, dehydroindigo and leucoindigo

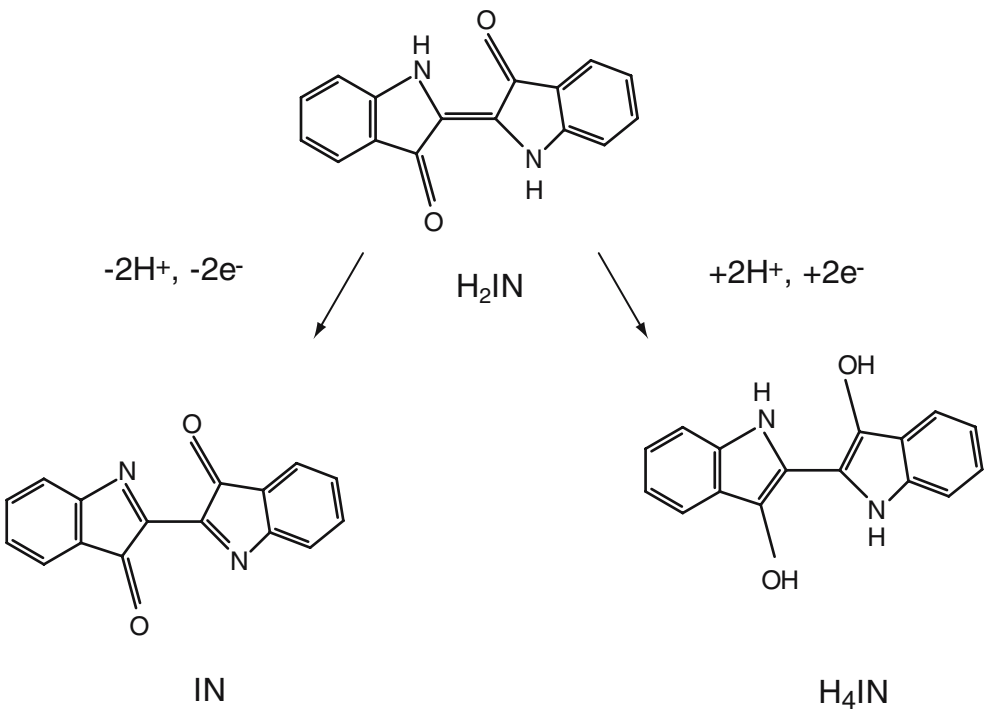

charge transfer through the solid particle occurs by means of electron hopping between adjacent molecules and involves the ingress/issue of electrolyte cations in/from the solid. Prior data for indigo microparticles suggest that proton hopping is restricted to a shallow boundary region of the crystals [52].

The SQWV response of indican and isatan B is illustrated in Fig. 2 for indican. As shown in Fig. 2a, on initiating the potential scan of −650 mV in the positive direction, a main oxidation process at +615 mV (III) is recorded. On initiating the potential at +850 mV in the positive direction, peaks at +445 (I) and −305 mV (II) accompanied by several weak peaks appear, as shown in Fig. 2b. Upon repetitive cycling of the potential scan, SQWVs reduce to those obtained for indigo microparticles, thus denoting that a conversion indican/indigo occurs.

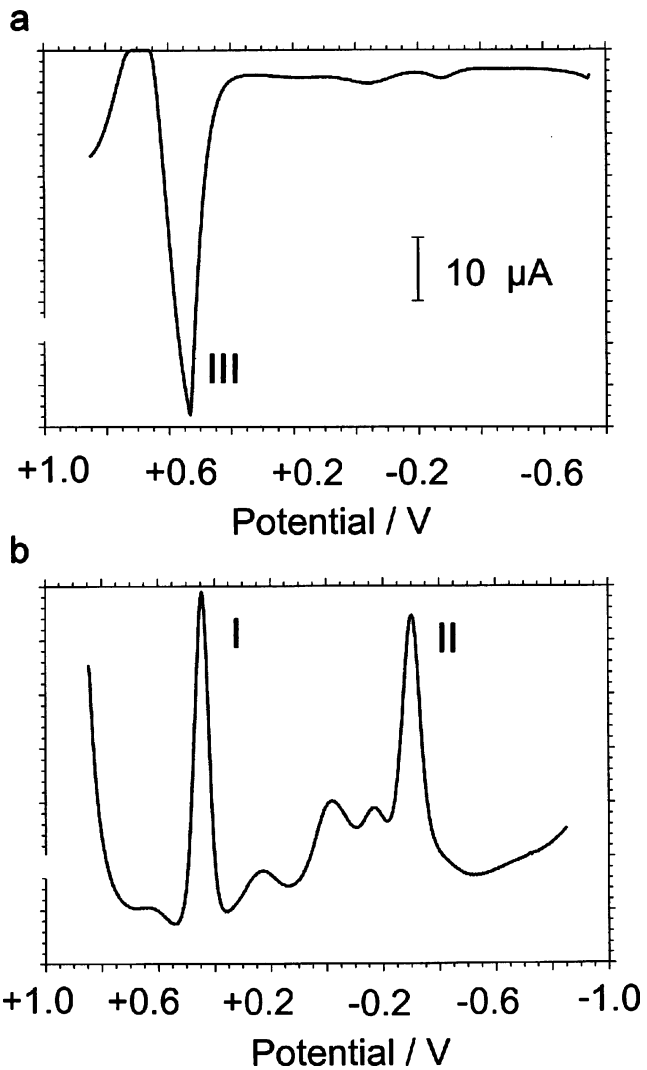

Fig. 2 SQWVs of indican-modified PIGE immersed into 0.50 M HAc+0.50 M NaAc buffer at pH 4.85. **a** Potential scan initiated at −650 mV in the positive direction; **b** id. at +850 mV in the negative direction. Potential step increment 4 mV; square wave amplitude 25 mV; frequency 15 Hz

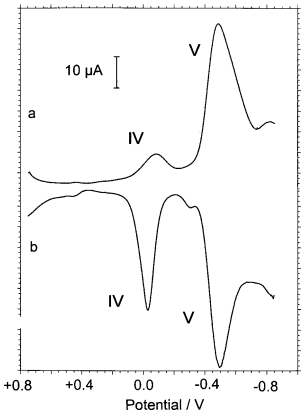

Fig. 3 SQWVs of isatin-modified PIGEs immersed into 0.50 M HAc+0.50 M NaAc buffer at pH 4.85. *a*, Potential scan initiated at +850 mV in the negative direction; *b*, potential scan initiated at −850 mV in the positive direction. Potential step increment 4 mV; square wave amplitude 25 mV; frequency 5 Hz

Repetitive voltammetry provides the increase in peaks I and II at the expense of peak III.

SQWVs of isatin and indirubin consisted, as depicted in Fig. 3, of two nearly reversible peaks at −15 (IV) and −450 mV (V). In repetitive voltammetry, the peak V increases at the expense of the peak IV, thus suggesting the occurrence of a coupled chemical reaction between the two electron transfer processes.

The electrochemical process III recorded for indicant and isatan can be attributed to the oxidation of such compounds (both represented as 2R–O–HIN) to indigo with loss of the glycoside moiety presumably as a diglycoside. This can be described as:

$$2(\mathrm{R-O-HIN})(\mathrm{s}) + \mathrm{H_2O} \rightarrow \mathrm{H_2IN(s)} + \mathrm{R-O-R(aq)} + 4\mathrm{H^+(aq)} + 4\mathrm{e^-} \quad (3)$$

A plausible representation of this electrochemical process is depicted in the Scheme 3.

The electrochemical process IV should correspond to the reduction in isatin, $HINO_2$, to its hydroxylated analogue, $HIN(OH)_2$ (see Scheme 4). This species rapidly dehydrates and condensates to give indirubin, H_2INR, further reduced to leucoindirubin, H_4INR. These processes can be represented by means of the equations:

$$\mathrm{HINO_2(s)} + 2\mathrm{H^+(aq)} + 2\mathrm{e^-} \rightarrow \mathrm{HIN(OH)_2(s)} \quad (4)$$

$$2\mathrm{HIN(OH)_2(s)} \rightarrow \mathrm{H_2INR(s)} + 2\mathrm{H_2O} \quad (5)$$

$$\mathrm{H_2INR(s)} + 2\mathrm{H^+(aq)} + 2\mathrm{e^-} \rightarrow \mathrm{H_4INR(s)} \quad (6)$$

This scheme is consistent with electrochemical data in the solution phase [53].

Electrochemistry of indigo specimens

As previously noted, characterisation of indigo formation from plants is uneasy because indigo precursors are

Scheme 3 Electrochemical oxidation of indican and isatans

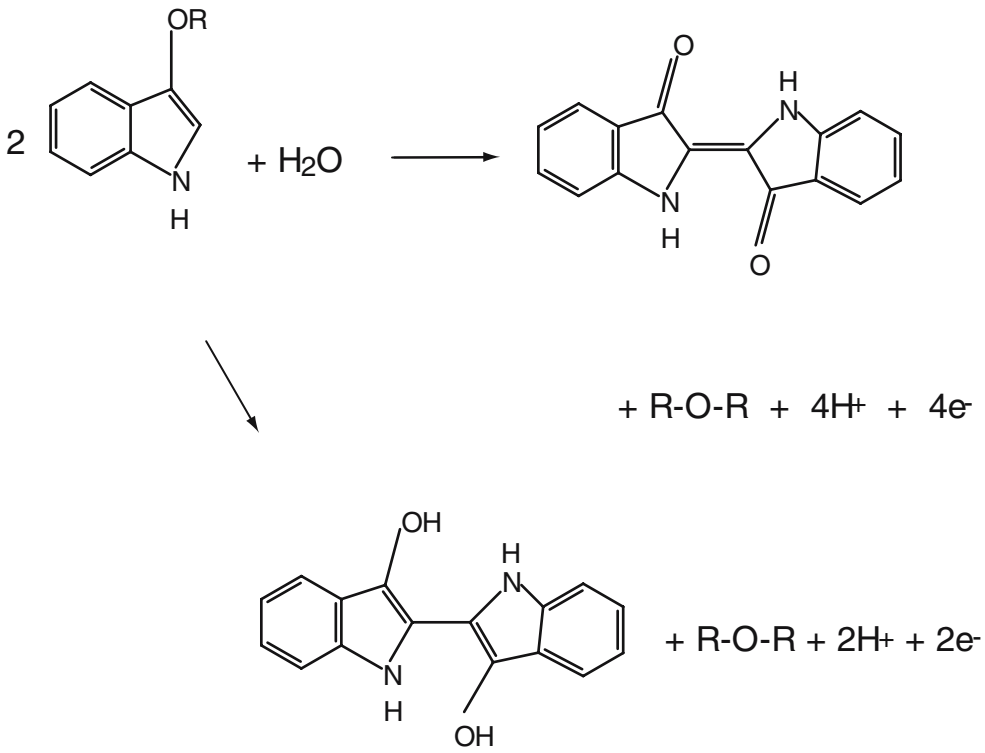

unstable compounds, difficult to isolate and purify [18–21]. Further, it should be noted that the quantity of indigo precursors in plant extracts is dependent on the species and the harvest period. In fact, isantans A and B disappear when the leaf material is subjected to a conventional drying process [21]. For this reason, voltammograms were taken for solid fractions of the beating suspension at different times during the process of traditional preparation of indigo, after drying partly with a filter paper ('wet' samples). A second series of measurements was performed after drying during 1 week (see "Experimental").

The evolution of the electrochemical response of 'wet' samples during the traditional preparation of indigo from *I. suffruticosa* leaves is depicted in Fig. 4 where SQWVs of the powders separated from the beating suspension at: (a) 6 and (b) 24 h (samples V-2 and V-4, respectively) of beating are shown. A yellow–greenish powder was first obtained whose voltammogram (Fig. 4a) presents a peaks at −300 (II), +100, +325 (VI), +450 (I) and +600 mV (III). On prolonging the beating process, a dark green powder was obtained for which the indigo-centred peaks I and II increase at the expense of all other signals (see Fig. 4b). In these voltammograms, isatan- and indican-characteristic (III) peaks are accompanied by an additional peak at +325 mV (VI). This peak is attributable to the two-proton, two-electron oxidation of indoxyl depicted in Scheme 4, another compound related with indigo precursors [15–21],

$$\mathrm{HIN(OH)(s)} \rightarrow \mathrm{INO(s)2H^{+}(aq)+2e^{-}} \quad (7)$$

as judged by the value of the peak potential compared with reported indoxyl derivatives [54]. Upon exhaustive drying of specimens (samples VD-1 to VD-6), indigo-centred peaks become increasingly marked, whereas all other peaks almost entirely disappear as can be seen in Fig. 4c for VD-6.

This electrochemical response is close to that recorded for some commercial indigos, shown in Fig. 5, for which, apart from peaks I and II, other well-defined peaks appear. Thus, indigo prepared from *Isatis tinctoria* (Fig. 5a), *Indigofera tinctoria* (Fig. 5b) and *I. suffruticosa* (sample VD-4, Fig. 5c) exhibit peaks at −425 (V) and approx. 0 mV (IV), attributable to traces of indirubin. The presence of such additional peaks allows for characterizing the indigo source using the peak current ratios for processes I, II, IV and V.

Voltammetry of MB samples

Typical SQWVs of MB samples are shown in Fig. 6, corresponding to (a) pristine palygorskite and MB samples from (b) Chacmultún and (c) El Tabasqueño, both dated in the Late Classical Maya period, immersed into acetate buffer at pH 4.85.

Because the amount of indigo in palygorkite is estimated between 1–3% (w/w) [4–8], MB samples provide weak indigo-centred peaks I and II accompanied by relatively large background peaks. These last signals are attributable to quinone functionalities produced in the graphite surface [57, 58], being promoted by scratching of the graphite surface during the process of electrode modification.

Scheme 4 Redox processes involved in the indoxyl/isatin/indirubin/leucoindirubin reaction path

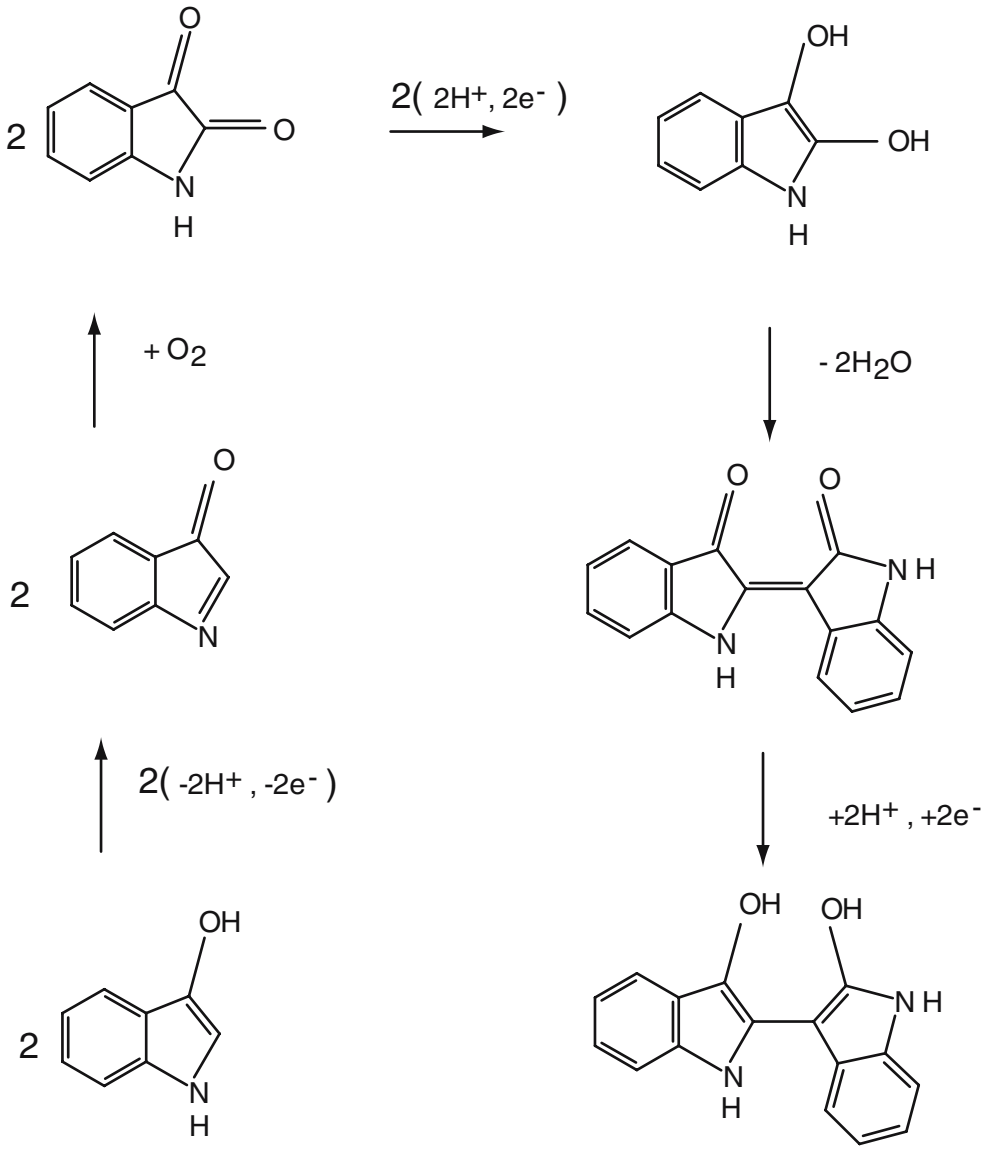

Accordingly, relatively intense 'scratching' peaks are recorded under our experimental conditions.

As previously described [22], peaks I and II in MB samples are wider than those recorded for indigo microparticles and exhibit light peak potential shifts (20–50 mV) with respect to the later. However, both peaks behave reversibly, as denoted by the independence of peak potentials on the frequency and the record of well-developed anodic and cathodic components of the square wave current [47].

Interestingly, peaks I and II are accompanied in several samples (see Fig. 6b) by a peak V at −450 mV, whereas in other cases, this peak is absent (Fig. 6c). Peak V can be attributed to the presence of indirubin, formed as a secondary product during the preparation of indigo. Differences observed between the scratching peaks in Fig. 6a–c can be attributed to the presence of variable amounts of silica and/or clays and, in particular, calcium carbonate (*vide infra*), which are absent in pristine palygorskite but existing in MB samples.

Discussion

As previously described [22], the quotient between the peak current of the processes I and II, $i_p(I)/i_p(II)$, can be taken as representative of the relation between the amounts of indigo, dehydroindigo and leucoindigo. The value of the $i_p(I)/i_p(II)$ ratio depends on the starting potential, frequency and square wave amplitude and differs significantly from indigo microparticles to MB samples as can be seen in Fig. 7, where the variation of the $i_p(I)/i_p(II)$ ratio at a potential step increment of 4 mV and a frequency of 15 Hz on the square wave amplitude, E_{SW}; is shown. As can be

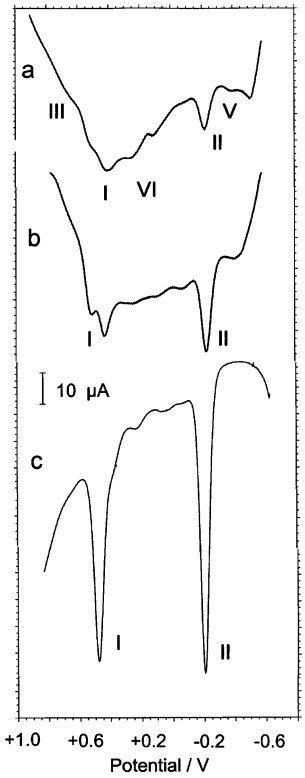

Fig. 4 SQWVs of PIGEs modified with samples separated from the suspension during the preparation of indigo from *Indigofera suffruticosa* leaves after: *a,* 'wet' sample V-2; *b*, 'wet' sample V-4; and *c*, 'dry' sample VD-6. Electrolyte 0.50 M HAc +0.50 M NaAc buffer at pH 4.85. Potential scan initiated at −650 mV in the positive direction. Potential step increment 4 mV; square wave amplitude 25 mV; frequency 15 Hz

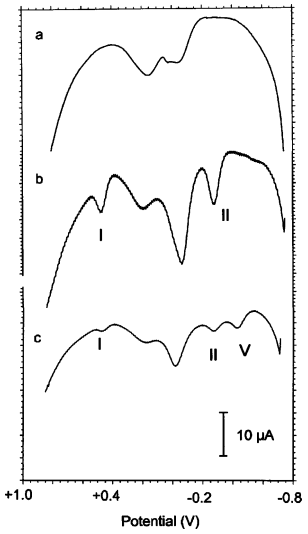

Fig. 6 SQWVs of PIGEs modified with pristine palygorskite from Sak lu'um (*a*) and MB samples from Chacumultún (*b*) and El Tabasqueño (*c*), immersed into 0.50 M HAc+ 0.50 M NaAc buffer at pH 4.85. Potential scan initiated at −750 mV in the positive direction. Potential step increment 4 mV; square wave amplitude 25 mV; frequency 5 Hz

seen in this figure, the $i_p(I)/i_p(II)$ ratio remains essentially E_{SW} independent for synthetic indigo. A similar behaviour with almost identical peak current values was obtained for commercial indigos and 'dried' samples VD-1 to VD-6. In contrast, MB samples provided larger $i_p(I)/i_p(II)$ ratios, particularly low square wave amplitudes. As can be seen in Fig. 7, 'wet' samples V-1 to V-6 (and VD-1 to VD-6) provided $i_p(I)/i_p(II)$ values intermediate to those obtained for synthetic indigo and MB samples, the peak current ratio approaching that of synthetic indigo on prolonging the beating time.

To quantify separately the dehydroindigo/indigo and indigo/leucoindigo ratios in samples, experimental voltammetric data were compared with theoretical cyclic voltammetric curves for systems containing simultaneous both the oxidised and reduced forms of the depolariser in different concentrations [55, 56]. The relevant point to emphasise is that the voltammetric profile is significantly dependent on

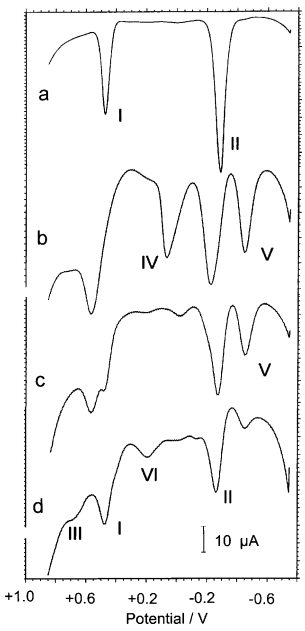

Fig. 5 SQWVs of PIGEs modified with indigo from different sources. *a*, Synthetic indigo; *b*, commercial indigo from *Isatis tinctoria*; *c*, commercial indigo from *Indigofera tinctoria*; *d*, indigo prepared from *Indigofera suffruticosa* (sample VD-4). Electrolyte 0.50 M HAc+ 0.50 M NaAc buffer at pH 4.85. Potential scan initiated at −750 mV in the positive direction. Potential step increment 4 mV; square wave amplitude 25 mV; frequency 15 Hz

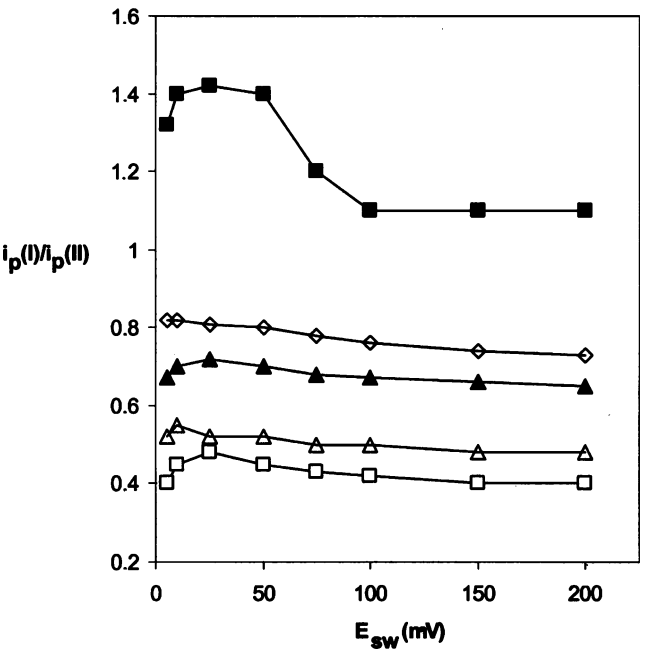

Fig. 7 Variation of the $i_p(I)/i_p(II)$ ratio with the square wave amplitude, E_{SW}, for indigo microparticles (*solid squares*), Maya Blue from the archaeological site of El Tabasqueño (Campeche, Late Classical Maya period, *squares*), 'wet' samples V-1 (*rhombs*) and V-4 (*solid triangles*) and 'dry' sample V-4 (*triangles*). From SQWVs recorded in acetate buffer initiated at −650 mV in the positive direction. Potential step increment 4 mV; frequency 5 Hz

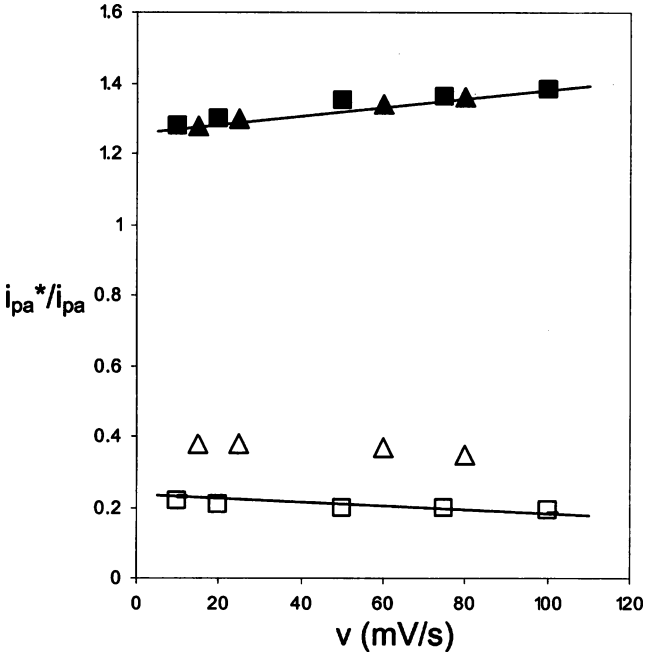

Fig. 8 Experimental data and theoretical values of the i_{pa}^*/i_{pa} ratio in CVs initiated at the formal electrode potential of each couple in the positive direction recorded at different potential scan rates for peaks I (*solid figures*) and II (*empty figures*). Electrode modifiers: synthetic indigo (*squares*) and sample V-2 (*triangles*). Theoretical lines for $\alpha_{red}=1$ (*upper*) and $\alpha_{red}=0$ (*low*)

the oxidised form/reduced form ratio, the potential scan rate and the starting potential and direction of the potential scan.

Application of one of the aforementioned methods is illustrated in Fig. 8. In this figure, the peak currents for the anodic peak are recorded in the first (i_{pa}^*) and the second (i_{pa}) scans when the voltammogram is initiated at the formal electrode potential of the couple in the positive direction of potentials. Because large background currents are obtained, base lines defined by the voltammetric curve before and after the voltammetric peak were used [56]. Experimental data and theoretical variations of (i_{pa}^*/i_{pa}) on the potential scan rate, v, for process I in CVs of synthetic indigo (solid squares) and sample V-2 (solid triangles) are shown. In both cases, experimental data fit with theory for a molar fraction of reduced form, α_{red}—in an hypothetical indigo+dehydroindigo mixture—equal to one. Data for process II corresponding to indigo (squares) and sample V-2 (triangles) are also shown in Fig. 8. For indigo, the molar fraction of reduced form in an hypothetical indigo+leucoindigo is now equal to 0. However, data for peak II in sample V-2 fits with theory for a molar fraction of indigo close to 0.80, thus denoting that a significant amount of leucoindigo exists ($\alpha_{red}=0.20$). Similar results were obtained using the method devised by Scholz and Hermes [55] (see Electronic supplementary materials).

The foregoing set of considerations is in agreement with spectral VIS and FTIR data. Thus, VIS spectra of samples exhibited absorption bands at 3,800 and 6,030 Å, common to indican and isatans [21]. This last is superimposed with the characteristic band of indigo which appears at a deltamax of 6,060 Å. This band increases at the expense of the band at 3,080 Å along each one of the V-1/V-6 and VD-1/VD-6 series, in agreement with the idea that indigo is progressively formed upon prolonging the beating process.

As can be seen in Fig. 9a, the ATR/FTIR spectrum of indigo shows a multiple-band profile with a sharp band at 1,630 cm^{-1}, characteristic of the carbonyl groups [23]. This band can also be seen in the spectra of dried samples after treatment with HCl, as shown in Fig. 9b. This treatment is needed for removing prominent carbonate bands resulting from calcium carbonate existing as a result of the maceration process of *Indigofera* leaves with quick lime, a situation common with MB samples [22] (see Electronic supplementary materials). Remarkably, no absorption band at 1,736 cm^{-1}, typical of dehydroindigo [23], was recorded in VD samples, thus denoting that this compound is not formed during the traditional preparation of indigo.

Such data suggest that during the traditional synthesis of indigo, its reduced form, leucoindigo, is initially formed in a significant amount, being further oxidised to indigo along the beating process. This is favoured by the alkaline quick-lime suspension in which the preparation is performed, because leucoindigo is slightly soluble in alkaline media [15–17]. The traditional synthesis of indigo implies,

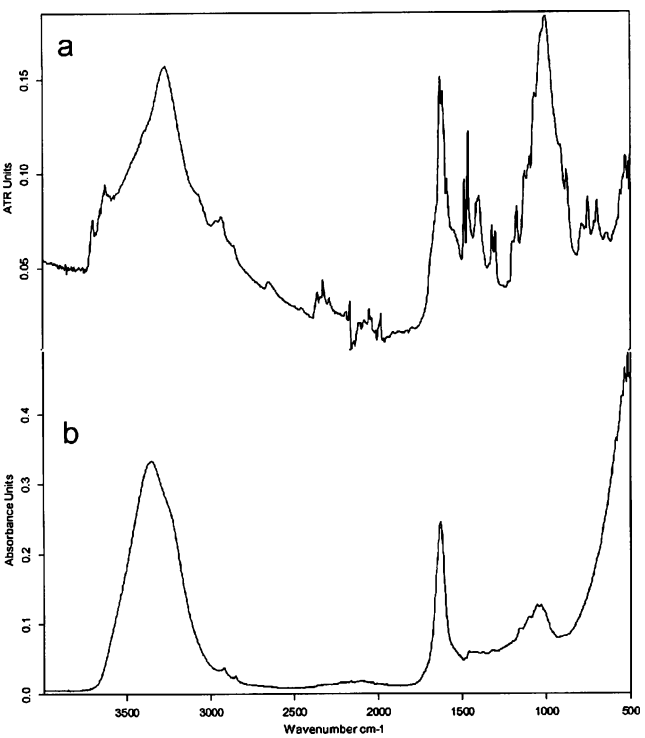

Fig. 9 FTIR/ATR spectra of synthetic indigo (*a*) and (*b*) sample VD-6 after treatment with HCl

Scheme 5 Possible scheme for the formation of indigo and indirubin from isatin/indican precursors

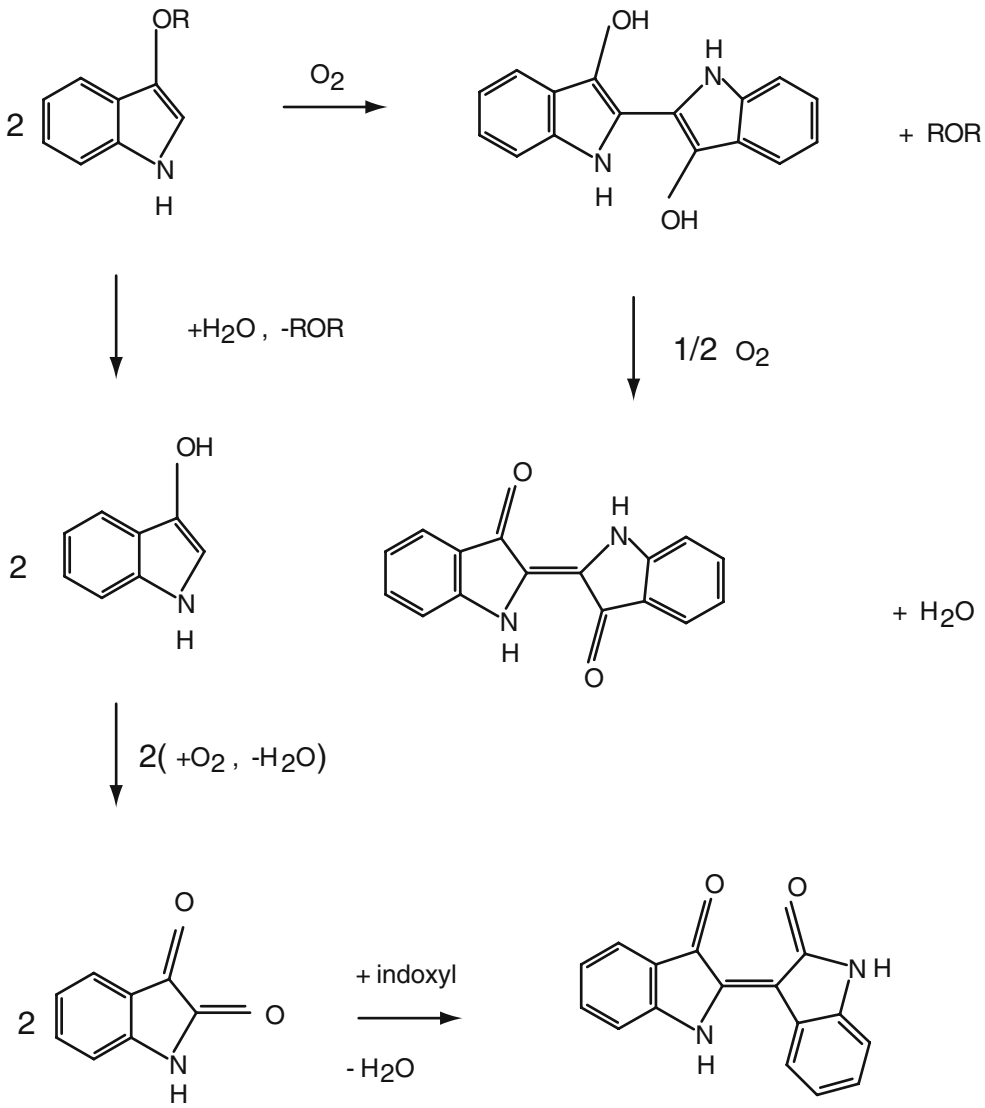

Table 1 Chronological and geographical scheme for MB samples that showed or not showed the indirubin-centred peak V

Period	Site	Peak V	No peak V
Postclassical	Mayapán		••••
Terminal Classical	Chichén Itzá		••••
	D'zula		•••
Late	Ek Balam	•	
	Dzibilnocac		♦♦
Classical	Kulubá	•	
	Chacmultún	•	
	Mulchic	•	••••
	El Tabasqueño	♦♦♦♦	•
	Acanceh	••	
Early Classical	Calakmul A6	♦♦	
Late Preclassical	Calakmul IIC	♦	

Circles, Yucatán sites; *rhombs*, Campeche sites

however, a relatively complicated pathway in which, apparently, indigo precursors slowly produce different indigo forms. Consistently, with recently proposed reaction schemes in plants [33–35], the first step of Maya's indigo production involves the hydrolysis of indican/isatan to indoxyl. This species undergoes at least two competing pathways; by the first token, leucoindigo—sligthtly soluble in alcaline media—is formed, being further oxidised to indigo through the beating process. The aerobic oxidation of indican and isatans can be represented as:

$$2(\mathrm{R-OHIN})(s) + \mathrm{O_2} \rightarrow \mathrm{H_4IN}(aq) + (\mathrm{R-O-R})(aq) \quad (8)$$

$$2\mathrm{H_4IN}(aq) + \mathrm{O_2} \rightarrow 2\mathrm{H_2IN}(s) + 2\mathrm{H_2O} \quad (9)$$

By the second, isatin is formed, further yielding indirubin via reaction between isatin and indoxyl. The reaction above

the pathways, starting from indican and isatans, are represented in Scheme 5.

The presence of indirubin in several MB samples and its absence in others can be either attributed to the following: (1) the use of different vegetal sources for indigo preparation, (2) the use of different preparation procedures of indigo and (3) the use of different procedures for indigo attachment to palygorskite. At the expense of a more detailed knowledge of the preparation of MB from indigo and palygorskite, our data suggest that different preparation procedures of indigo were used by the ancient Mayas. As can be seen in Table 1, the time distribution of MB samples containing and not containing indirubin presents a significant regularity. In contrast, no comparable regularity is obtained with regard to the geographical distribution of samples.

As can be seen in Table 1, indirubin-containing MB samples are grouped in ancient archaeological sites, whereas the indirubin-free ones are largely concentrated in the more recent sites. Because the indirubin/indigotin ratio appears to be highly sensitive on the indigo source and preparation procedure, the above features suggest that the ancient Mayas evolved their preparation recipes along time. Additionally, our data suggest that this technological change occurred during the Late Classical period.

Final considerations

The solid-state voltammetry of samples taken from aqueous lime suspensions obtained at different stages during the traditional preparation of indigo from *I. suffruticosa* leaves produces well-defined responses that can be attributed to indigo and accompanying compounds.

Reported data suggest that the preparation of indigo following Maya's ancient procedures is initiated by the hydrolysis of isatans and indican to isatin and indoxyl, yielding indigo and eventually indirubin. Prolonged beating in contact with the air results in an exhaustive conversion of leucoindigo into indigo, whereas the drying process eliminates unstable indigo precursors. No significant amounts of dehydroindigo were found during the preparation of indigo using traditional procedures. This implies that the conversion of indigo into dehydroindigo attributed to MB is a palygorskite-supported process, so that ancient Mayas initiated the synthesis of hybrid inorganic–organic materials.

The absence/presence of indirubin accompanying indigo in MB samples denotes that the ancient Mayas used probably different preparation procedures (and/or eventually different vegetal sources) for indigo and/or MB from indigo and palygorskite. This preparation procedure changed probably during the Late Classical Maya period, thus denoting that the technology of this ancient culture evolved significantly along time.

Acknowledgements Financial support is gratefully acknowledged from the Generalitat Valenciana I+D+I project AE06/131.

References

1. Romero P, Sánchez, C (2005) New J Chem 29:57
2. José-Yacamán M, Rendón L, Arenas J, Serra Puche MC (1996) Science 273:223
3. Polette LA, Meitzner G, José-Yacamán M, Chianelli RR (2002) Microchem J 71:167
4. Chiari G, Giustetto R, Riccihiardi G (2003) Eur J Mineral 15:21
5. Fois E, Gamba A, Tilocca A (2003) Microporous Mesoporous Mater 57:263
6. Hubbard B, Kuang W, Moser A, Facey GA, Detellier C (2003) Clay Miner 51:318
7. Witke K, Brzezinka K-W, Lamprecht I (2003) J Mol Struct 661–662:235
8. del Río MS, Martinetto P, Somogyi A, Reyes-Valerio C, Dooryhée E, Peltier N, Alianelli L, Moignard B, Pichon L, Calligaro T, Dran J-C (2004) Spectrochim Acta Part B 59:1619
9. Reinen D, Köhl P, Müller C (2004) Z Anorg Allg Chem 630:97
10. Chianelli RR, Perez de la Rosa M, Meitzner G, Siadati M, Berhault G, Mehta A, Pople J, Fuentes S, Alonzo-Nuñez G, Polette LA (2005) J Synchroton Radiat 12:129
11. del Rio MS, Sodo A, Eeckhout SG, Neisius T, Martinetto P, Dooryhee E, Reyes-Valerio C (2005) Nucl Instrum Methods Phys Res B 238:50
12. Giustetto R, Llabres i Xamena FX, Ricchiardi G, Bordiga S, Damin A, Gobetto R, Chierotti MR (2005) J Phys Chem B 109:19360
13. Kleber R, Masschelein-Kleiner L, Tissen J (1967) Stud Conserv 12:41
14. Vandenabeele P, Bode S, Alonso A, Moens L (2005) Spectrochim Acta Part A 61A:2349
15. Eller-Pandraud HV (1959) Comptes Rendus 248:2581
16. Kokubun T, Edmonds J, John P (1998) Phytochemistry 48:1
17. Margaud T, Enaud E, Choisy P, Legoy MD (2001) Phytochemistry 58:897
18. Gilbert KG, Hill DJ, Crespo C, Mas A, Lewis MJ, Rudolph B, Cooke DT (2000) Phytochem Anal 11:18
19. Oberthuer C, Schneider B, Graf H, Hamburger M (2004) Chem Biodiversity 1:174
20. Gilbert KG, Maule HG, Rudolph B, Lewis M, Vandenburg H, Sales E, Tozzi S, Cooke DT (2004) Biotechnol Prog 20:1289
21. Oberthür C, Graf H, Hambuerger M (2004) Phytochemistry 65:3261
22. Doménech A, Doménech MT, Vázquez ML (2006) J Phys Chem B 110:6027
23. Klessinger M, Luettke W (1963) Tetrahedron 19(suppl 2):315
24. Magaloni Kerpel D (1996) Materiales y técnicas de la pintura Maya. Facultad de Filosofía y Letras, Universidad Nacional Autónoma de México
25. Tagle A, Paschinger H, Richard H, Infante G (1990) Stud Conserv 35:156
26. Reyes-Valerio C (1993) De Bonampak al Templo Mayor: el azul Maya en Mesoamérica, Siglo XXI, Madrid
27. Torres LM (1998) Mater Res Soc Symp Proc 123
28. Orska-Gawrys J, Surowiec I, Kehl J, Rejniak H, Urbaniak-Walczak K, Trojanowicz M (2003) J Chromatogr A 989:239
29. Szostek B, Orska-Gawrys J, Surowiec I, Trojanowicz M (2003) J Chromatogr A 1012:179

30. Puchalska M, Polec-Pawlak K, Zadrozna I, Hryszko H, Jarosz M (2004) J Mass Spectrom 39:1441
31. Andreotti A, Bonaduce I, Colombini MP, Ribechini E (2004) Rapid Commun Mass Spectrom 18:1213
32. Vandeabeele P (2003) Analyst 128:187
33. Betchold T, Turcanu A, Geissler S, Ganglberger E (2002) Bioresour Technol 81:171
34. Berry A, Dodge TC, Pepsin M, Weyler W (2002) J Ind Microbiol Biotech 28:127
35. Ferreira ESB, Hulme AN, McNab H, Quye A (2004) Chem Soc Rev 33:329
36. Scholz F, Nitschke L, Henrion G (1989) Naturwissenschaften 76:71
37. Scholz F, Nitschke L, Henrion G, Damaschun F (1989) Naturwiss 76:167
38. Scholz F, Meyer B (1998) In: Bard AJ, Rubinstein I (eds) Electroanalytical chemistry, a series of advances, vol 20. Marcel Dekker, New York, p 1
39. Grygar T, Marken F, Schröder U, Scholz F (2002) Collect Czechoslov Chem Commun 67:63
40. Scholz F, Nitschke L, Henrion G, Fresenius Z (1989) Anal Chem 334:56
41. Jaworski A, Stojek Z, Scholz F (1993) J Electroanal Chem 354:1
42. Komorsky-Lovric S, Mircevski V, Scholz F (1999) Mikrochim Acta 132:67
43. Doménech A, Doménech MT, Saurí MC, Gimeno JV, Bosch F (2003) Anal Bioanal Chem 375:1161
44. Grygar T, Kucková S, Hradil D, Hradilová D (2003) J Solid State Electrochem 7:706
45. Doménech A, Doménech MT, Saurí MC (2005) Talanta 66:769
46. Bond AM, Marken F, Hill E, Compton RG, Hügel H (1997) J Chem Soc Perkin Trans 2:1735
47. Lovric M (2002) In: Scholz F (ed) Electroanalytical methods. Springer, Berlin, p 111
48. Lovric M, Scholz F (1997) J Solid State Electrochem 1:108
49. Lovric M, Scholz F (1999) J Solid State Electrochem 3:172
50. Oldham KB (1998) J Solid State Electrochem 2:367
51. Schröder U, Oldham KB, Myland JC, Mahon PJ, Scholz F (2000) J Solid State Electrochem 4:314
52. Doménech A, Doménech MT (2006) J Solid State Electrochem 10:459
53. Khattab MA, Ghoneim MM (1983) J Indian Chem Soc 60:643
54. Fernández C, Costa A (1998) Electroanalysis 10:249
55. Scholz F, Hermes M (1999) Electrochem Commun 1:345
56. Doménech A, Sánchez S, Doménech MT, Gimeno JV, Bosch F, Yusá DJ, Saurí MC (2002) Electroanalysis 14:685
57. Barisci JN, Wallace GG, Baughman RH (2000) Electrochim Acta 46:509
58. Barisci JN, Wallace GG, Baughman RH (2000) J Electroanal Chem 488:92